Available online at www.sciencedirect.com
ScienceDirect
International Journal of Pharmaceutics 351 (2008) 23–30
INTERNATIONAL JOURNAL OF PHARMACEUTICS
www.elsevier.com/locate/ijpharm

Characterizing molar mass distributions and molecule structures of different chitosans using asymmetrical flow field-flow fractionation combined with multi-angle light scattering

Christian Augsten, Karsten Mäder *

Institute of Pharmaceutics and Biopharmaceutics, Wolfgang-Langenbeck-Str. 4, D-06120 Halle/Saale, Martin-Luther-University Halle-Wittenberg, Germany

Received 21 November 2006; received in revised form 11 September 2007; accepted 13 September 2007
Available online 18 September 2007

Abstract

We investigated various chitosan types and batches successfully with a combination of asymmetrical flow field-flow fractionation and multi-angle light scattering using a customized separation method. Advantageous were the separation capability of a broad applicable molar mass range, the injection of unpurified solutions and the determination of absolute molar masses. Most of the measured samples followed molar mass distributions of monomodal logarithmic Gaussian type. Only one sample showed a very broad distribution caused by either high molar mass amounts or aggregate formation. It was also found that batch-to-batch variations were quite high, which is a common problem for nature-derived products. Thus, especially pharmaceutical products and semi-synthetic derivates should benefit from the development of products with a predictable average molar mass and a narrow distribution. On the basis of received data for each slice eluting from the channel, molar mass–gyration radius relationships could be generated for every single measurement. The hereof received molecule structure parameters were verified to be molar mass dependent, ranging from open structures of rinsed thoroughly molecules to theta coil conditions or an even more compact conformation.

Keywords: Chitosan; Field-flow fractionation; Multi-angle light scattering (MALS); Molecular weight; Molar mass distribution; Molecular structure

1. Introduction

The aim of our study was to separate aqueous acidic solutions of different chitosan types by asymmetrical flow field-flow fractionation (aFlow-FFF or AF4). We characterized them in detail by directly connected multi-angle light scattering (MALS) and refractive index (RI) detectors (aFlow-FFF/MALS/RI). Furthermore several batches of the same type were investigated to check batch-to-batch consistency.

1.1. Chitosan

An increasing number of publications about chitosan and its derivates show the growing importance of this substance. In the case of pharmaceutical purposes this is supported by a new monograph of chitosan hydrochloride (European Pharmacopoeia, 2005) and descriptions in other pharmaceutical books (Holpert, 1999). Several reviews and book chapters are highlightening the structure and various applications of chitosan (Peter, 2005; Illum, 1998; Felt et al., 1998).

Chitosan is a linear polymer that is known to be non-toxic. Its structure is given in Fig. 1. It is a naturally polyaminosaccharide composed of *N*-acetylglucosamine (GlcNAc) and glucosamine (GlcN) residues. The monomer units are linked via β-1.4-glycosidic bonds. Several producers use the term "degree of (de)acetylation" to describe the relationship of both monomer fractions in their products. Furthermore the F_A value was suggested (Roberts, 1997) that is representing the GlcNAc residue mole fraction of the polymer. Ideal chitin would represent an F_A of 1.0 and ideal chitosan of F_A 0.0 whereas most producers offer chitosans with $0 \leq F_A \leq 0.2$. Chitosan is soluble in acidic solutions as, e.g. 1% aqueous acetic acid due to its pK_a between 6.2 and 6.4. The technology of chitosan production

* Corresponding author at: Institut für Pharm. Technologie, Wolfgang-Langenbeck-Straße 4, 06120 Halle, Germany. Tel.: +49 345 5525167; fax: +49 345 5527029.
E-mail address: karsten.maeder@pharmazie.uni-halle.de (K. Mäder).

0378-5173/$ – see front matter © 2007 Elsevier B.V. All rights reserved.
doi:10.1016/j.ijpharm.2007.09.013

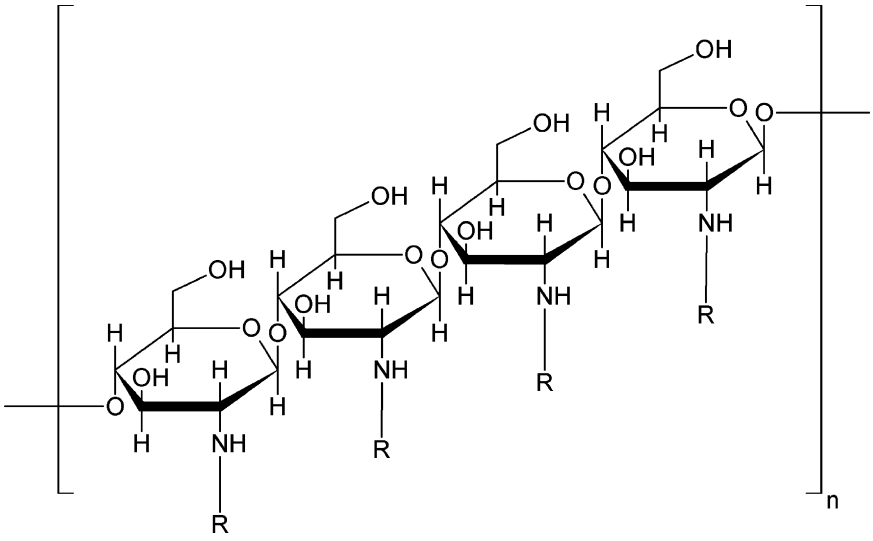

Fig. 1. Structure of chitosan, R = H (GlcN) and in low amounts R = Ac (GlcNAc).

is well known. It is achieved from different chitin containing material as exoskeletons of arthropoda and many plants and fungi. The preparation procedures were reviewed in detail (No and Myers, 1997). Principally, the waste fractions from shellfish industry as crabs and shrimps are deprotonized, demineralized, decolorized and deacetylated. According to the comment corresponding to the monograph of chitosan hydrochloride (European Pharmacopoeia, 2005), the most important resulting quality parameters are (de)acetylation degree, molar mass (distribution) and impurity content, especially of proteins and heavy metals. All these parameters depend on the material natural sources and on the process parameters. In addition, molar mass and F_A value influence each other. A more complete deacetylation causes a more excessive depolymerization. Thus, it is difficult for producers to offer exactly the same product properties over a longer time or from batch to batch.

However, products of the same F_A type and with defined molar mass distributions are desired due to the influence on a lot of important parameters. For example, molar mass has an effect on viscosities of aqueous solutions. Viscosity differences achieve greater importance if chitosans are used as stabilizers and thickeners in acidic media or in hydrogel formulations. This field of application is advantageously due to the bacterial growth prevention what was also found to be molar mass dependent (Zivanovic et al., 2004). Currently, chitosan is not registered by the FDA as a drug for the treatment of diseases. But in pharmaceutics it is used as a new excipient in tablets and pellets or as a drug carrier in micro- and nanoparticles (Kato et al., 2003; Hoepfner et al., 2002). Furthermore chitosan is mucoadhesive and applied in wound dressing and transmucosal drug delivery. Other fields of application are bone regeneration and fat emulsification because of its lipid-binding properties. Due to its polycationic nature it interacts with negatively charged tissue surfaces and macromolecules. Thus, recently it achieved increasing importance because of its DNA complexation potential (Mansouri et al., 2004). The molar mass can have influence on important properties within this field as, e.g. shown for blood plasma levels of DNA delivery systems (Richardson et al., 1999). Chitosan is also achieving growing importance as a base material to create new chemical modified derivates, several of them are listed elsewhere (Peter, 2005). The molar mass is an important value to characterize the initial substance and to achieve a resulting product of desired properties. One example of the influence of molar mass is given for mucoadhesive potential of thiolated chitosans as oral controlled drug delivery systems (Roldo et al., 2004).

1.2. Molar mass determination methods used before for chitosan

In most cases, only viscosity values in strongly acidic solutions are provided in sheets of commercially available products. Viscosities can be used to calculate average molar mass values. However, this procedure is not an absolute method and gives only an approximation of the molar mass. It is not capable to describe molar mass distributions or polydispersities, which are required to assure a constant product quality. Therefore, alternative methods are necessary.

Another possibility is mass spectrometry (MS). However, chitosan is difficult to analyze due to its polycationic nature and broad molar mass distribution including high molar mass components. MS was successfully used to characterize low molar mass degradation products of chitosan, but not for the parent chitosan molecule (Bahrke et al., 2002).

Another option is the use of a stand-alone static light scattering detector. Nevertheless received values are depended on the sample preparation procedure due to the presence of small amounts of aggregates that were previously described by various authors. The aggregates influence the light scattering signal, resulting in non-reliable molar mass determinations (Anthonsen et al., 1994).

GPC is commonly used in polymer characterization. Advantageously a pre-equilibrium-dialysis of polysaccharides is not necessary. But in the case of chitosans unsolvable aggregates

Table 1
Chitosan types and batches from Primex Ingredients, Island

Abbreviation	A	B	C	D1	D2	D3
Name	Chitosan FG 80	Chitosan FG 85	Chitosan FG 90	Chitoclear FG 95	Chitoclear FG 95	Chitoclear FG 95
Batch	TM661	TM611	TD132	TM1885	TM 1360	TM 1369
Deacetylation [%][a]	80.8	87.7	90.7	99	96	95
Viscosity [cP][a,b]	36	10	59	78	16	51

[a] Values given by the producer.
[b] For 1% in 1% acetic acid.

should be removed before characterization even when large pore-size gels are used. Additionally irreversible adsorption of sample components can occur at some columns and has to be avoided. Because of the lack of chitosan standards and calibration with dextrans, furthermore the molar mass of chitosans may be overestimated. A GPC/MALS combination (Beri et al., 1993; Ottoy et al., 1996) is more favourably but not solving all GPC problems (Varum and Smidsrod, 2005).

1.3. Molar mass determination using Flow-FFF/MALS

Flow-FFF/MALS has become a recent alternative to GPC/MALS. This combination of both techniques was already successfully applied to various macromolecular substances for pharmaceutical purposes (Fraunhofer and Winter, 2004). Several polysaccharides have been separated in the past. Examples include pullulans and dextrans (Wittgren and Wahlund, 1997) or κ-carrageenan and xanthan (Viebke and Williams, 2000). Surprisingly, only one application note (Johann, 2004) without any detailed description of fractionation or analysis procedure describes the characterization of chitosan. The main advantage of Flow-FFF is the broad separation range from 10^3 to above 10^7 Da and the better separation of polymers greater than approximately 5×10^4 g/mol in contrast to GPC (Hansen and Klein, 2001). That is advantageously for the characterization of chitosans that are known to be polydisperse with respect to molar mass (Ottoy et al., 1996). Additionally for Flow-FFF aggregate containing samples must not be prefiltered and can be injected directly.

The field-flow fractionation (FFF) principles and method family are summarized elsewhere (Giddings, 1968, 1993). Using the submethod asymmetrical flow field-flow fractionation (aFlow-FFF), molecules or particles are separated with regard to their hydrodynamic sizes in the central part of the apparatus, the channel (Wahlund and Giddings, 1987). Using the Flow-FFF theory, from the sample retention time the diffusion coefficient and subsequently the hydrodynamic diameter can be calculated (Schure et al., 2000; Dondi and Martin, 2000).

But this calculation can be difficult if not impossible due to various sample–membrane interactions, zone spreading or overloading phenomena inside the channel (Cölfen and Antonietti, 2000). Especially polyelectrolytes are known to cause several problems. Thus, coupling Flow-FFF to molar mass detectors as MALS is an optimal option. Due to this combination, no reference standards are necessary and absolute molar masses and gyration radii (r_g) can be calculated for each slice eluting from the separation channel. A detailed overview of basic theories for MALS data evaluations can be found elsewhere (Wyatt, 1993, 1998).

2. Materials and methods

Samples of different commercial types and batches of chitosan from Primex Ingredients (Siglufjordur, Iceland) were used. They are given in Table 1. An acetate buffer consisting of 4.57 g/l acetic acid and 1.96 g/l sodium acetate (pH 4.2) according to Beri was used (Beri et al., 1993). The solution contained also 0.2 g/l sodium azide to prevent bacterial growth.

The samples were separated using asymmetrical Flow-FFF and characterized using MALS and refractive index (RI) detectors. The characterization equipment consisted of the channel, Eclipse F and the 18 angle scattering detector Dawn EOS from Wyatt Technology Europe. An RI detector from Shodex (RI-101) was used. The system was tested with dextran 65 kDa to check separation and molar mass determination capability. Using a dn/dc value of 0.150 ml/g, a weight averaged molar mass of 67 kDa was achieved. After several experiments to optimize separation, a method was developed for characterization of chitosans covering a wide range of molar mass. The following parameters were used for all separations: The detector flow was kept constant at 1 ml/min. After flow equilibrium, a volume of 100 μl of the respective 2 mg/ml chitosan solution was injected with 0.2 ml/min for 2 min while focusing and focused further for 1 min with 2 ml/min focus flow. During elution, the cross flow was kept for 2 min at a flow rate of 2 ml/min, The cross flow rate decreased in the following 5 min linearly to 1 ml/min and in the following 17 min from 1 ml/min to 0 ml/min. This two step cross-flow rate gradient was necessary to separate all the sample content in adequate time due to the high polydispersity of the samples. The separation started at 6 min and ended at approximately 30 min. A channel spacer of a height of 350 μm was used. The membrane consisted of regenerated cellulose with a cut-off of 10^4 g/mol (Nadir C010F, Microdyn-Nadir GmbH). To determine average values, the scattering and concentration data was evaluated using the Astra 4.9 software (Wyatt Technology Corporation). Mean values of molar masses and polydispersities were calculated using the Zimm equation with a detector fit degree of 1. Given error bars correspond to the statistical uncertainties given by the Astra program covering all evaluated sample slice data. For differential plots and Flory exponent determinations the molar mass and radius data were fitted via polynomial fourth degree. A refractive index increment of 0.181 ml/g was used for highly deacetylated chitosans in acetate buffer of pH 4.2 according to Beri et al. (1993).

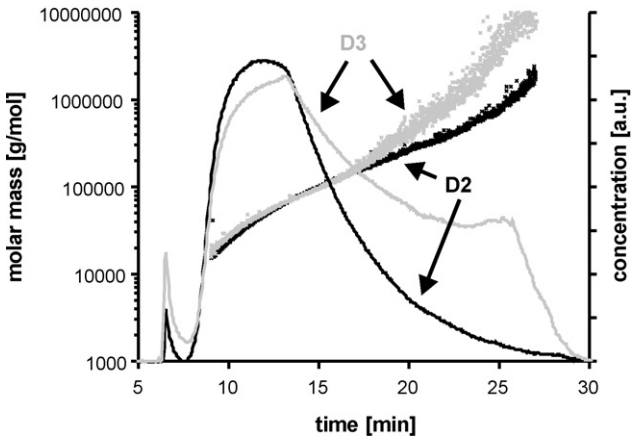

Fig. 2. Fractograms of chitosan D2 and D3, concentrations (line) and molar masses (dots).

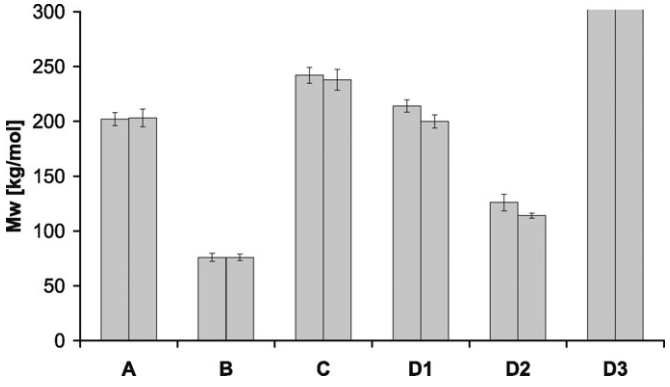

Fig. 4. Weight average molar masses (M_w) of all chitosan types, determined from light scattering (values of chitosan D3 are $1.3 \pm 0.2 \times 10^6$ and $1.4 \pm 0.3 \times 10^6$ g/mol).

The intrinsic viscosities were determined using Ubbelohde viscosimeters (Schott, type 0a and I) for chitosan solutions from 0.05 to 0.3% (w/v) at a temperature of 25 °C. The outlet time results were slightly adjusted via Hagenbach correction to consider the amount of potential energy that is needed to accelerate the liquid. The liquid densities were determined using a Mohr-Westphal weighing machine (Johannes Hammer, Germany). Further evaluation procedures are described at respective position in the following text.

3. Results and discussion

3.1. Influence of chitosan type and batch

Asymmetrical Flow-FFF/MALS/RI provided concentration and absolute molar masses for each of the sample slices eluting from the channel. Although always the same separation method was used, all chitosan types revealed different elution behaviours. The fractograms of D2 and D3 chitosan types are exemplarily given in Fig. 2. At a time of approximately 6–7 min the Flow-FFF characteristic void peak could be seen. It was followed by the actual chitosan concentration peak at higher elution times up to above 20 min. All chitosan fractograms exhibited only one peak, except of D3. According to FFF theory, generally molecules of lower molar masses eluted faster from the channel. We expected that at least the three chitosans of same type but different batches, D1, D2 and D3, would show similar fractograms. However, this was not the case.

Average molar mass values were calculated from MALS and RI data. The corresponding information is given in Figs. 3 and 4. The number average molar masses of all chitosans covered values between approximately 4×10^4 and 1×10^5 g/mol. The weight average molar masses were higher due to the polydispersity of the samples. The lowest values resulted for B and D2. Both chitosans also represented fractogram signals mainly located at lower elution times what was in accordance with the Flow-FFF separation principle. Furthermore, the corresponding values in Figs. 3 and 4 proved the differences between D1, D2 and D3.

From the relationship M_w/M_n the PDI values in Fig. 5 between approximately 1.8 and 2.8 were received for most chitosans. Similar or slightly higher values were reported by Varum (Varum et al., 2005). The three batches D1, D2 and D3 showed quite different PDI values. Thus, their different product qualities were proved by their average molar masses and molar mass distributions, indicating a high batch-to-batch variability. Therefore, the development of new products or the application of fractionated samples might be necessary as in the field of pharmaceutics predictable product properties are required, which are related to a narrow mass distribution.

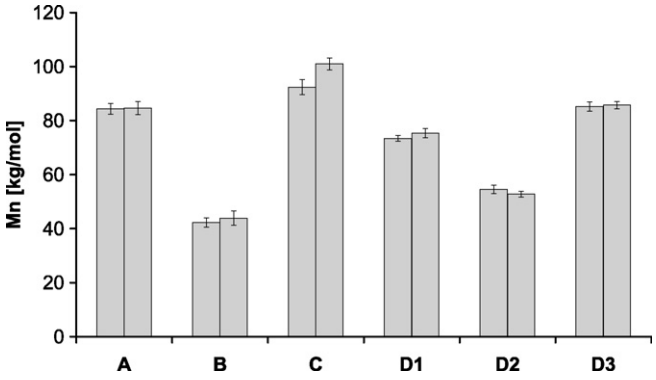

Fig. 3. Number average molar masses (M_n) of all chitosan types, determined from light scattering.

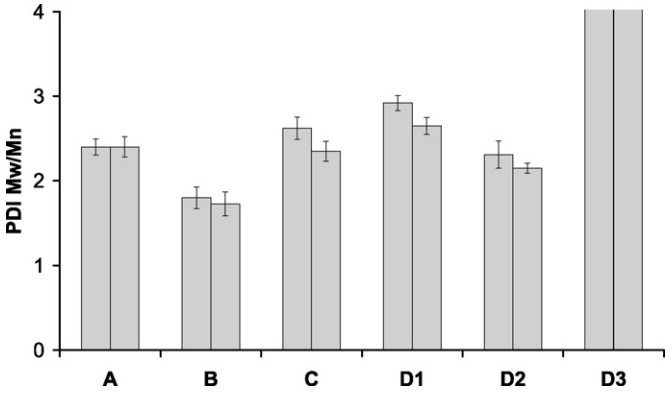

Fig. 5. Polydispersity values (PDI) of all chitosan types, determined from light scattering (values of chitosan D3 are 15 ± 3 and 17 ± 3).

Table 2
Influence of molar mass fit method on average values of example measurements of chitosan B, D1 and D3

Formalism	Zimm[a]	Debye[a]	Random coil
Chitosan B			
M_w [kg/mol]	76	72	73
M_n [kg/mol]	42	42	42
PDI	1.80	1.72	1.72
Chitosan D1			
M_w [kg/mol]	200	175	192
M_n [kg/mol]	75	74	75
PDI	2.65	2.35	2.56
Chitosan D3			
M_w [kg/mol]	1284	540	1068
M_n [kg/mol]	85	84	85
PDI	15.07	6.47	12.61

[a] Detector fit degree = 1.

Due to the natural origin, a PDI below approximately 2 is difficult to achieve for raw material without fractionation but a PDI of approximately 3 should possibly not be exceeded. The extraordinary high two-digit PDI value for chitosan D3 resulted from its high weight average molar mass exceeding 10^6 g/mol. This value could be explained by the high molar mass fraction representing the second peak at approximately 25 min in its fractogram (Fig. 2). Several other chitosan types also reached molar mass values of around 10^6 g/mol at the end of elution but their concentration quantity was less pronounced. This difference can be also seen in the differential curves in Fig. 6. Nearly all chitosans were able to be fitted to a monomodal logarithmic Gauss distribution. Only the sample D3 exhibited a non-monomodal plot reaching molar masses of approximately 1×10^7 g/mol. To apply Gaussian model on D3, a mass distribution over three peaks had to be assumed. Another explanation for D3 would be the appearance of aggregates in solution what was already detected for highly acetylated chitosans (Ottoy et al., 1996).

However, this high molar mass fraction of the second fractogram peak made the selection of one MALS fit method for average calculation difficult. Table 2 is giving the influence of three usable formalisms. Chitosan B with its narrow distribution (PDI 1.80, Zimm) gave quite similar M_w values for all three fits, while D1 with its broader distribution (PDI 2.65, Zimm) resulted in slightly differences. Due to the second peak of D3, all three methods resulted in relatively high M_w and high PDI values. Thus, both values were proved to be much higher for D3 compared to the other chitosans but the results varied enormously depending on the formalism. Therefore, the molar mass values of chitosan D3 were handled with care and not taken as absolute values. Compared to M_w, the number averaged molar mass values M_n were less influenced by the selected calculation method and seem therefore better suited for a comparison of the examined chitosan types.

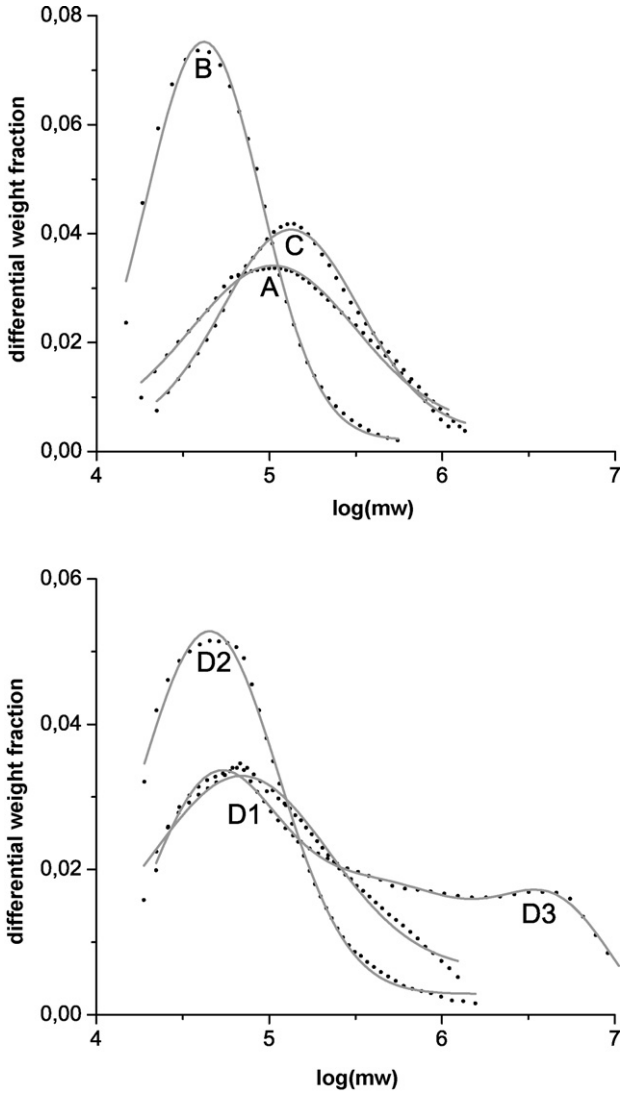

Fig. 6. Differential weight fraction versus log(M_w) plots of all chitosan types with single peak Gaussian fits (for D3: triple peak Gaussian fit), determined from light scattering.

The recovery rates and gyration radii of all chitosans are given in Table 3. The r_g values increased with increasing molar mass.

Table 3
Recovery rates determined from RI signal and weight average gyration radii $\langle r_g \rangle_w$ determined from light scattering of all chitosan types

	Chitosan					
	A	B	C	D1	D2	D3[a]
$\langle r_g \rangle_w$ [nm]	50.2 ± 4% 52.9 ± 5%	29.5 ± 23% 23.8 ± 23%	61.8 ± 3% 60.2 ± 4%	54.7 ± 3% 49.5 ± 4%	34.3 ± 8% 34.5 ± 5%	99.4 ± 8% 99.1 ± 8%
Recovery [%]	89.5 94.8	85.1 82.0	95.9 91.2	94.1 90.3	87.9 83.1	107.9 107.3

[a] Data evaluation difficult due to the second fractogram peak.

Table 4
Values of Flory exponent ν, Mark–Houwink exponent α and mass fractal dimension D_m for several ideal structures ranging from sphere (closed structure) to rod (open structure)

Structure	α	ν	D_m
Ideal sphere (no polymer)	0	0.33	3
Polymer θ coil/disk	0.5	0.5	2
Polymer in good solvent	1	0.67	1.5
Ideal rod (no polymer)	2	1	1

The recovery rates indicated that most of the samples eluted within separation time and thus channel membrane was selected correct to prevent excessive absorption.

3.2. Chitosan conformation in solution

In addition to molar masses, it is important to receive knowledge about conformation of the chitosan macromolecules in solution. Usually for polysaccharide characterization the intrinsic viscosity $[\eta]$ and the molar mass are connected via the Mark–Houwink–Kuhn–Sekurada (MHKS) equation (Berth and Dautzenberg, 1998),

$$[\eta] = k_\alpha M_v^\alpha$$

where k_α is a constant that is related to the polymer–solvent system. M_v is the viscosity average molar mass but can be exchanged with the weight average molar mass M_w. The MHKS exponent α is classified in Table 4. Common values are 0.5 for linear chain molecules forming a θ coil what is the case in relatively bad solvents and rinsed thoroughly molecule coils resulting in a value of 1.

Fig. 7 is giving the intrinsic viscosities in dependence of weight average molar mass as a double logarithmic plot. The determined intrinsic viscosities covered a similar range as chitosan values reported in other acidic solutions, e.g. Anthonsen et al. (1993). The MHKS equation corresponding to the data in Fig. 7 was

$$[\eta] = 0.039 M_w^{0.81} \quad \text{with} \quad R^2 = 0.986$$

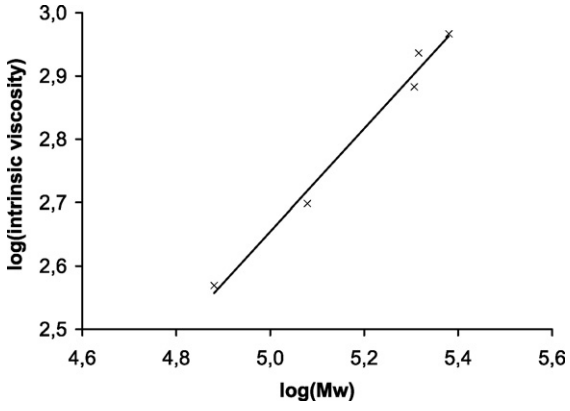

Fig. 7. Double logarithmic plot of intrinsic viscosity $[\eta]$ versus weight average molar mass M_w, corresponding regression line $\log[\eta] = 0.81 \times \log(M_w) - 1.41$ with $R^2 = 0.986$, single values are $[\eta]_A = 764 \pm 12$ ml/g, $[\eta]_B = 371 \pm 14$ ml/g, $[\eta]_C = 926 \pm 57$ ml/g, $[\eta]_{D1} = 864 \pm 3$ ml/g, $[\eta]_{D2} = 499 \pm 9$ ml/g, D3 neglected due to its difficult molar mass determination.

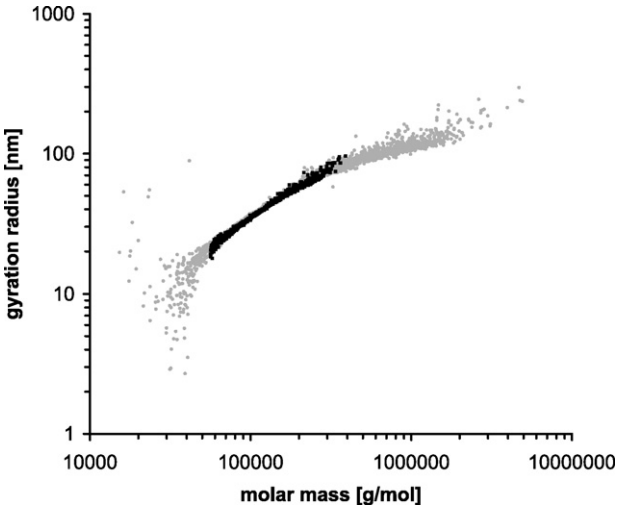

Fig. 8. Double logarithmic plot of molar mass versus gyration radius of chitosan C, selected region for linearization marked black.

The α value of 0.81 represented more a random coil-like polymer in a good solvent than a molecule structure of an ideal θ coil. Thus, the used acetate buffer of pH 4.2 was a relatively good solvent for these highly deacetylated chitosans. A comparison to literature is difficult, as already pointed out by other authors (Varum et al., 2005). Chemical composition, molar mass and ionic strength are only some parameters influencing characterization. Several other authors found in acidic solutions increasing MHKS exponents with increasing F_A (Anthonsen et al., 1993; Ottoy et al., 1996; Fee et al., 2003; Lamarque et al., 2005). In contrast, a deacetylation independent α value of 0.92 was calculated (Berth et al., 2002). However, the measured value of 0.81 is comparable to the ones determined in similar acidic media for chitosans of comparable F_A.

The disadvantage of this method is the necessary high number of substances of different molar masses. If a molar mass dependent molecule structures exist, they can be hardly recognized by this technique. As described for other polysaccharides characterized by a Flow-FFF/MALS combination (Wittgren and Wahlund, 1997), also the equation can be used relating weight average molar mass M_w and gyration radius $\langle r_g^2 \rangle^{1/2}$ that is mostly simplified as r_g,

$$\left\langle r_g^2 \right\rangle^{1/2} = k_\nu M_w^\nu$$

where k_ν is a constant with similar dependencies as k_α.

Polysaccharides are mostly broad distributed polymers. Thus, the Flory exponent ν can be calculated from the slope of a double logarithmic plot of M_w versus r_g of only one sample measurement. In the case of chitosans, the middle range was interesting and therefore used for ν calculation, as given in Fig. 8. For small molecules below $\lambda/20$ no reliable size data was calculable due to the laser wavelength λ of 690 nm. For molecules exceeding approximately 300 kDa, the application of Zimm equation for size calculation was difficult. The Flory exponent ν can be converted into the mass fractal dimension D_m via

$$D_m = \frac{1}{\nu}$$

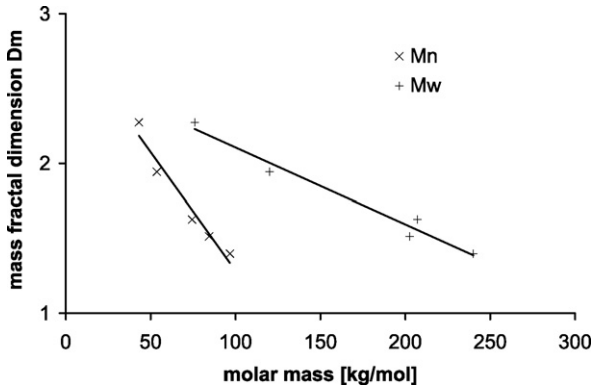

Fig. 9. Average molar masses M_n or M_w versus mass fractal dimensions D_m (chitosan D3 neglected due to its difficult molar mass determination).

Both values can give information about the openness of the molecule structure. For ideal structures they can be connected with the MHKS exponent via (Thielking and Kulicke, 1996):

$$\alpha = 3\nu - 1$$

Table 4 is providing an overview of all form parameters for ideal structures. The determined chitosan α value of 0.81 corresponded to a theoretical D_m value of 1.65. In comparison, the D_m values revealed by Flow-FFF/MALS are given in Fig. 9. The average of all samples represented a D_m of 1.75 what was slightly higher but nearly matched the predicted value from viscosity measurements. A comparison to the previous literature is difficult due to the diversity of findings which is probably caused by the different used chitosan qualities and solvents. From a collection of several chitosan measurements a deacetylation independent α value of 0.92 and a ν value of 0.55 were calculated what corresponds to a theoretical D_m of 1.56 or 1.81 (Berth et al., 2002). This discrepancy was explained by a draining effect of chain conformation. We received values in a similar range and also of a small difference supporting the general structure assumption, although the relationship from Flory to MHKS exponent was less distinctive. But the individual light scattering dependent values in Fig. 9 diverged from the average in the range from 1.40 to 2.27. This can be interpreted as a molar mass dependent openness of the molecule in solution. The higher the average molar mass values were, the lower D_m values were achieved. No mathematical description can be found in the literature. The linear regression lines were

$$D_m = -1.58 \times 10^{-5}\,(\mathrm{mol/g})\,M_n + 2.87 \quad \text{with} \quad R^2 = 0.958$$
$$D_m = -5.1 \times 10^{-6}\,(\mathrm{mol/g})\,M_w + 2.62 \quad \text{with} \quad R^2 = 0.971$$

The reason for this solution behaviour is still unexplained. In contrast to the structure values we revealed with Flow-FFF/MALS, other authors have combined several measurements of chitosans differing in molar mass by using, e.g. different raw material (Cölfen et al., 2001) or degradation (Anthonsen et al., 1994) or reacetylation products (Lamarque et al., 2005). In contrast to (Berth et al., 2002), most of them found that ν is deacetylation dependent and smaller for products of lower F_A. It ranged from values in the region of θ coil condition to the ones corresponding to good solvents. A dependency of F_A was not given in our measurements, but understandably due to the used chitosans in similar deacetylation range. In contrast, Flory exponents for each single chitosan were given by (Beri et al., 1993) for the same solvent of pH 4.2 we used. But they questioned their own values due to the low sample polydispersity and the exceptionally low ν values. This makes a comparison to our findings not recommendable.

However, our determined values covered a wide range of ν values that can also be found for similar acidic solvents in literature. Our findings revealed an additional molar mass dependency of ν. This effect should be taken into account in the future. Further tests might show if this is also valid for chitosans of other molar mass ranges in solvents of varying pH and ionic strength. Thus, in the case of chitosan we suggest to determine the α and ν exponents preferably by measuring values for each single sample by a separation method as Flow-FFF combined with a MALS or a viscosity detector. This equipment can be used to give additional information compared to determinations of the molecule structure by series of different molar mass samples.

3.3. Conclusion

Chitosan is a polysaccharide with growing importance for several purposes. The importance of molar mass is known for many applications and especially critical in the field of pharmaceutics. Flow-FFF with a MALS detector is a new and until now rarely used combination for polysaccharide characterization.

This technique was successfully applied to various commercial chitosan types and batches. The equipment was found to be advantageous due to the separation capability of a broad applicable molar mass range including detection of high molar mass fractions or aggregates. Furthermore unpurified samples could be injected and absolute molar masses were calculated. The elution behaviour was found to be molar mass dependent, supported by values calculated from scattering signal. The measured average molar masses and their distributions suggested that the batch-to-batch variations were quite high. Most chitosans showed monomodal logarithmic Gaussian mass distributions. Only one chitosan batch contained either high molar mass chains or aggregates resulting in a very broad molar mass distribution. Therefore, a prediction of product properties is questionable and an application in pharmaceutics cannot be advised. Certainly these product quality variations were dedicated to the strong dependence of natural origin of chitosan. Thus, pharmaceutical products and semi-synthetic derivates should benefit from the development of chitosans with a predictable average molar mass and a narrow distribution. Commonly provided viscosity values are no sufficient criteria for characterizing chitosan product properties. Instead of this, a pretesting of every batch before use is advantageous where Flow-FFF/MALS is an ideal tool for chitosan characterization.

Furthermore most chitosans allowed calculation of structure information from the relationship of molar mass and molecule viscosity or size data. Light scattering based, the detected molar mass dependent structure relationship ranged from macromolecules rinsed thoroughly to molecules with a relatively compact conformation. For the future, a molar mass depen-

dency of molecule structure of chitosans should be taken into account.

Acknowledgements

The authors express their thanks to Primex Marine Biotechnology that kindly donated the chitosans and especially to Dr. Roessner from Wyatt Technology Europe and Dr. habil. Katharina Maria Picker-Freyer for the helpful discussions. Furthermore we want to thank Mrs. Todte for her support for the viscosity measurements.

References

Anthonsen, M.W., Varum, K.M., Hermansson, A.M., Smidsrod, O., Brant, D.A., 1994. Aggregates in acidic solutions of chitosans detected by static laser light scattering. Carbohydr. Polym. 25, 13–23.

Anthonsen, M.W., Varum, K.M., Smidsrod, O., 1993. Solution properties of chitosans: conformation and chain stiffness of chitosans with different degrees of *N*-acetylation. Carbohydr. Polym. 22, 193–201.

Bahrke, S., Einarsson, J.M., Gislason, J., Haebel, S., Letzel, M.C., Peter-Katalinic, J., Peter, M.G., 2002. Sequence analysis of chitooligosaccharides by matrix-assisted laser desorption ionization postsource decay mass spectrometry. Biomacromolecules 3, 696–704.

Beri, R.G., Walker, J., Reese, E.T., Rollings, J.E., 1993. Characterization of chitosans via coupled size-exclusion chromatography and multiple-angle laser light-scattering technique. Carbohydr. Res. 238, 11–26.

Berth, G., Cölfen, H., Dautzenberg, H., 2002. Physicochemical and chemical characterization of chitosan in dilute aqueous solution. Prog. Colloid Polym. Sci. 119, 50–57.

Berth, G., Dautzenberg, H., 1998. Solution behavior of some selected polysaccharides studied preferentially by static light scattering. Rec. Res. Dev. Macromol. Res. 3, 225–248.

Cölfen, H., Berth, G., Dautzenberg, H., 2001. Hydrodynamic studies on chitosans in aqueous solution. Carbohydr. Polym. 45, 373–383.

Cölfen, H., Antonietti, M., 2000. Field-flow fractionation techniques for polymer and colloid analysis. Adv. Polym. Sci. 150, 67–187.

Dondi, F., Martin, M., 2000. Physicochemical measurements and distributions from field-flow fractionation. In: Schimpf, M.E., Caldwell, K., Giddings, J.C. (Eds.), Field-flow-fractionation Handbook. Wiley Interscience, New York, pp. 103–132.

European Pharmacopoeia, 2005. 5th edition and corresponding comment of delivery 18. Deutscher Apotheker Verlag, Stuttgart, pp. 1728–1729.

Fee, M., Errington, N., Jumel, K., Illum, L., Smith, A., Harding, S.E., 2003. Correlation of SEC/MALS with ultracentrifuge and viscosimetric data for chitosans. Eur. Biophys. J. 32, 457–464.

Felt, O., Buri, P., Gurny, R., 1998. Chitosan: a unique polysaccharide for drug delivery. Drug Dev. Ind. Pharm. 24, 979–993.

Fraunhofer, W., Winter, G., 2004. The use of asymmetrical flow field-flow fractionation in pharmaceutics and biopharmaceutics. Eur. J. Pharm. Biopharm. 58, 369–383.

Giddings, J.C., 1968. Nonequilibrium theory of field-flow fractionation. J. Chem. Phys. 49, 81–86.

Giddings, J.C., 1993. Field-flow fractionation: analysis of macromolecular, colloidal, and particulate materials. Science 260, 1456–1465.

Hansen, M., Klein, T., 2001. Feldflussfraktionierung—Das bestgehütete Geheimnis in der Bioanalytik? GIT Labor-Fachz. 5, 506–615.

Hoepfner, E.-M., Reng, A., Schmidt, P.C., 2002. Chitosan. In: Fiedler, H.P. (Ed.), Fiedler Lexikon der Hilfsstoffe für Pharmazie, Kosmetik und angrenzende Gebiete, fifth ed. E. Cantor Verlag, Aulendorf, pp. 423–427.

Holpert, C., 1999. Chitosanhydrochlorid. In: von Bruchhausen, F., Hackenthal, E., Holzgrabe, U. (Eds.), Hagers Handbuch der Pharmazeutischen Praxis, fifth ed. Springer-Verlag, Berlin, pp. 241–242.

Illum, L., 1998. Chitosan and its use as a pharmaceutical excipient. Pharm. Res. 15, 1326–1331.

Johann, C., 2004. Absolute macromolecular characterization with fractionation: a viable alternative to traditional separation methods. Am. Lab. 36, 12–14.

Kato, Y., Onishi, H., Machida, Y., 2003. Application of chitin and chitosan derivatives in the pharmaceutical field. Curr. Pharm. Biotechnol. 4, 303–309.

Lamarque, G., Lucas, J.-M., Viton, C., Domard, A., 2005. Physicochemical behavior of homogeneous series of acetylated chitosans in aqueous solution: role of various structural parameters. Biomacromolecules 6, 131–142.

Mansouri, S., Lavigne, P., Corsi, K., Benderdour, M., Beaumont, E., Fernandes, J.C., 2004. Chitosan-DNA nanoparticles as non-viral vectors in gene therapy: strategies to improve transfection efficacy. Eur. J. Pharm. Biopharm. 57, 1–8.

No, K.H., Myers, S.P., 1997. Preparation of chitin and chitosan. In: Muzzarelli, R.A.A., Peter, M.G. (Eds.), Chitin Handbook. Atec Edizioni, Grottammare, pp. 475–489.

Ottoy, M.H., Varum, K.M., Christensen, B.E., Anthonsen, M.W., Smidsrod, O., 1996. Preparative and analytical size-exclusion chromatography of chitosans. Carhohydr. Polym. 31, 253–261.

Peter, M.G., 2005. Chitin and chitosan from animal sources. In: Steinbüchel, A., Rhee, S.K. (Eds.), Polysaccharides: Polysaccharides and Polyamides in the Food Industry. Wiley-VCH Verlag, Weinheim, pp. 119–208.

Richardson, S.C.W., Kolbe, H.V.J., Duncan, R., 1999. Potential of low molecular mass chitosan as a DNA delivery system: biocompatibility, body distribution and ability to complex and protect DNA. Int. J. Pharm. 178, 231–243.

Roberts, G.A.F., 1997. Chitosan production routes and their role in determining the structure and properties of the product. Adv. Chit. Sci. 2, 22–31.

Roldo, M., Hornof, M., Caliceti, P., Bernkop-Schnürch, A., 2004. Mucoadhesive thiolated chitosans as platforms for oral controlled drug delivery: synthesis an in vitro evaluation. Eur. J. Pharm. Biopharm. 57, 115–121.

Schure, M.R., Schimpf, M.E., Schettler, P.D., 2000. Retention-normal mode. In: Schimpf, M.E., Caldwell, K., Giddings, J.C. (Eds.), Field-flow-fractionation Handbook. Wiley Interscience, New York, pp. 31–48.

Thielking, H., Kulicke, W.-M., 1996. On-line coupling of flow field-flow fractionation and multiangle laser light scattering for the characterization of macromolecules in aqueous solution as illustrated by sulfonated polystyrene samples. Anal. Chem. 68, 1169–1173.

Varum, K.M., Smidsrod, O., 2005. Structure-property relationship of chitosans. In: Dumitriu, S. (Ed.), Polysaccharides: Structural diversity and Functional Versatility, second ed. Dekker, New York, pp. 625–642.

Viebke, C., Williams, P.A., 2000. Determination of molecular mass distribution of κ-carrageenan and xanthan using asymmetrical flow field-flow fractionation. Food Hydrocolloid 14, 265–270.

Wahlund, K.-G., Giddings, J.C., 1987. Properties of an asymmetrical flow field-flow fractionation channel having one permeable wall. Anal. Chem. 59, 1332–1339.

Wittgren, B., Wahlund, K.-G., 1997. Fast molecular mass and size characterization of polysaccharides using asymmetrical flow field-flow fractionation—multiangle light scattering. J. Chromatogr. A 760, 205–218.

Wyatt, P.J., 1993. Light scattering and the absolute characterization of macromolecules. Anal. Chim. Acta 272, 1–40.

Wyatt, P.J., 1998. Submicrometer particle sizing by multiangle light scattering following fractionation. J. Colloid Interface Sci. 197, 9–20.

Zivanovic, S., Basurto, C.C., Chi, S., Davidson, P.M., Weiss, J., 2004. Molecular weight of chitosan influences antimicrobial activity in oil-in-water emulsions. J. Food Protect. 67, 952–959.